arXiv:1304.6143v1 [cond-mat.soft] 23 Apr 2013

Modeling Smectic Layers in Confined Geometries: Order Parameter and Defects

Mykhailo Y. Pevnyi and Jonathan V. Selinger*
Liquid Crystal Institute, Kent State University, Kent, Ohio 44242, USA

Timothy J. Sluckin
School of Mathematics, University of Southampton, Southampton SO17 1BJ, United Kingdom†
(Dated: April 22, 2013)

We identify a problem with the standard complex order parameter formalism for smectic-A (SmA) liquid crystals, which cannot describe certain types of physical defects, and discuss possible alternative descriptions of smectic order. In particular, we suggest an approach based on the real smectic density variation rather than a complex order parameter. This approach gives reasonable numerical results for the smectic layer configuration and director field in sample geometries, and can be used to model smectic liquid crystals under nanoscale confinement for technological applications.

For over forty years, theoretical understanding of smectic liquid crystals has been based on the complex order parameter $\psi(\mathbf{r})$ introduced by de Gennes [1, 2], which represents the magnitude and phase of layer ordering. During this time, the order parameter has been useful in many ways. It demonstrated an analogy between smectic liquid crystals and superconductors, allowing methods of solid-state physics to be applied to liquid-crystal science [1, 3]. It led to theories for the nematic-SmA and isotropic-SmA transitions, which are strongly affected by nematic order fluctuations [4–8]. It further led to prediction of twist-grain-boundary phases, liquid-crystal analogues of the Abrikosov flux lattice in type-II superconductors [9]. Most recently, it has led to calculations for smectic layer configurations in confined geometries [10–16], which may be useful for design of smectic devices [17].

The purpose of this paper is to point out a problem with the complex order parameter description, which affects some but certainly not all of the work that has been done with it. The complex order parameter is unable to describe certain types of defects that can realistically occur and hence, in some versions of the theory, it predicts unphysical configurations of smectic layers. We discuss theoretical approaches to resolve this problem, and use one of these approaches to calculate smectic layer configurations.

To see the problem, consider a disclination defect as in Fig. 1. In this figure, every point on the plane has a local density $\rho(\mathbf{r}) = \rho_0 + \delta\rho(\mathbf{r})$, with bright and dark regions corresponding to higher and lower density, respectively. To use the complex order parameter $\psi(\mathbf{r})$, we must write the local density variation, compared with the average ρ_0, as $\delta\rho(\mathbf{r}) = Re[\psi(\mathbf{r})]$. However, it is impossible to associate a unique complex number ψ with each point around the defect. If we try to make this association, then we must say that the phase of ψ increases downward in the lower-left quadrant, outward in the right half, upward in the upper-left quadrant, and eventually we reach an inconsistency. There must be a *branch cut* where ψ changes to the complex conjugate ψ^*, as illustrated by the dotted line. This situation is similar to the well-known problem of describing nematic order with a unit vector $\hat{\mathbf{n}}(\mathbf{r})$: going around a half-charge disclination, there must be a branch cut where $\hat{\mathbf{n}}$ changes to $-\hat{\mathbf{n}}$.

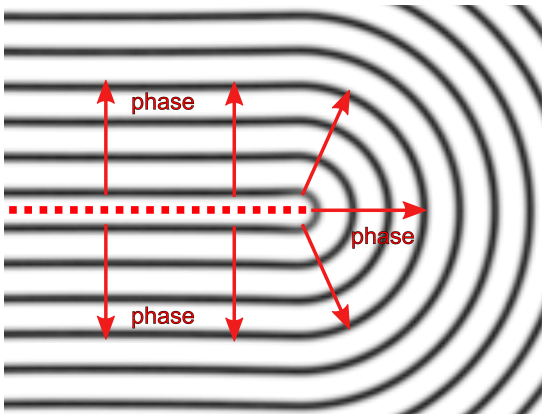

FIG. 1. Disclination in a two-dimensional smectic phase. Bright and dark regions correspond to higher and lower density, respectively, and the red dotted line is the branch cut in ψ and $\hat{\mathbf{n}}$.

The branch cuts in ψ and $\hat{\mathbf{n}}$ occur for the same physical reason: neither of these quantities gives an exactly correct description of the symmetry of the phase. The nematic phase has orientational order along the axis represented by $\pm\hat{\mathbf{n}}$, which can be described correctly by a tensor. The vector $\hat{\mathbf{n}}$ is often adequate as an approximate description, but the sign of $\hat{\mathbf{n}}$ does not correspond to anything physical. Hence, a branch cut in the sign of $\hat{\mathbf{n}}$ is not a physical defect, and it cannot cost any free energy. Likewise, the smectic phase has higher density at some positions and lower density at other positions, and this density variation can be described correctly by the real number $\delta\rho$ or $Re(\psi)$. The full complex number ψ may be mathematically convenient as an approximate description, but $Im(\psi)$ does not correspond to anything physical. Hence, a branch cut in $Im(\psi)$ is not a physical defect, and it cannot cost any free energy.

Does this issue with ψ affect any calculations? We

can see two situations with *no problem*. The first safe situation is if the nematic order is well aligned, so that there are no half-charged disclinations. For example, in a model for the nematic-smectic transition, the nematic order might be strong on both sides of the transition, with only small spin-wave fluctuations and no topological defects. In that case, ψ can describe the smectic order.

The second safe situation is if branch cuts in ψ and $\hat{\mathbf{n}}$ compensate for each other in the free energy. For example, de Gennes' original free energy density [1] can be written as

$$f = r|\psi|^2 + \frac{u}{2}|\psi|^4 + C|(\nabla - iq\hat{\mathbf{n}})\psi|^2 + f_N, \qquad (1)$$

where q is the favored wavevector of smectic order and f_N the nematic free energy density. This expression has a symmetry on changing $(\psi, \hat{\mathbf{n}}) \to (\psi^*, -\hat{\mathbf{n}})$, although it does not have symmetries on $\psi \to \psi^*$ or $\hat{\mathbf{n}} \to -\hat{\mathbf{n}}$ separately. Going around the disclination of Fig. 1, both ψ and $\hat{\mathbf{n}}$ have branch cuts, where $\hat{\mathbf{n}}$ is discontinuous and ψ has a discontinuous derivative. However, if the same branch cut is used for both variables, then the discontinuity in $\hat{\mathbf{n}}$ compensates for the discontinuity in $\nabla\psi$ in the derivative term of the free energy. As a result, the free energy is well-behaved with no singularity across the branch cut.

By contrast, in more recent theories of the isotropic-smectic transition [6–8], $\hat{\mathbf{n}}$ is replaced by the tensor order parameter $Q_{ij} = S(\frac{3}{2}n_i n_j - \frac{1}{2}\delta_{ij})$, and the free energy density is written as

$$f = \frac{1}{2}\alpha|\psi|^2 + \frac{1}{4}\beta|\psi|^4 + \frac{1}{2}\delta|\psi|^2 Q_{ij}Q_{ij} \qquad (2)$$
$$+\frac{1}{2}b_1|\nabla\psi|^2 + \frac{1}{2}b_2|\Delta\psi|^2 + \frac{1}{2}e_1 Q_{ij}\nabla_i\psi\nabla_j\psi^* + f_N.$$

In principle, working with Q_{ij} instead of $\hat{\mathbf{n}}$ should be an improvement, because Q_{ij} is uniquely defined everywhere. However, in this type of theory, there is no way to compensate for the branch cut in ψ. Hence, the free energy is singular along the branch cut, and it cannot describe physical defects as in Fig. 1. As a result, there is a risk that it might predict unphysical defects instead.

We can suggest three possible approaches to resolve this problem:

(1) We can go back to de Gennes' original free energy in terms of $\hat{\mathbf{n}}$ instead of Q_{ij}. In this approach, we must make sure that all physical quantities respect the symmetry $(\psi, \hat{\mathbf{n}}) \to (\psi^*, -\hat{\mathbf{n}})$, and have no singularity along a branch cut where ψ and $\hat{\mathbf{n}}$ both switch. For example, in a lattice or finite-element version of the model, we must be able to switch $(\psi, \hat{\mathbf{n}}) \to (\psi^*, -\hat{\mathbf{n}})$ on any single site, without making the switch on neighboring sites. In principle this calculation should be possible, but it is awkward to work with two unphysical quantities that compensate for each other, and hence we will not pursue it further.

(2) We can replace $\mathbf{n}$ by Q_{ij}, and replace ψ by a new type of mathematical object with the right symmetry. This is essentially the approach used by Alexander *et al.* [18, 19], who represent smectic order by a height function which includes both increasing and decreasing components simultaneously. Alternatively, we might represent smectic order by $\tilde{\psi} = Re(\psi) + i|Im(\psi)|$, which can be uniquely defined everywhere, with no branch cut. This calculation should be possible, but it is awkward to define a new type of mathematical object and work out the appropriate calculus for it. Hence, in this study we will not pursue that approach either.

(3) We can replace $\mathbf{n}$ by Q_{ij}, and replace ψ by the physical density variation $\delta\rho$. In that case, the theory becomes a form of density functional theory, analogous to early work on smectic phases [20, 21]. We find this approach the most physical and will use it for the rest of this article.

For this theory, we use a free energy density for the SmA phase of the form

$$f = \frac{a}{2}\delta\rho^2 + \frac{b}{3}\delta\rho^3 + \frac{c}{4}\delta\rho^4 + B\left[(\partial_i\partial_j + q^2 n_i n_j)\delta\rho\right]^2$$
$$+\frac{1}{2}K(\partial_i n_j)^2, \qquad (3)$$

where $\delta\rho(\mathbf{r})$ is the local deviation from the average density ρ_0. This model has a transition from the nematic phase when a is above a threshold to the SmA phase when a is below the threshold. In the SmA phase, the free energy minimum is approximately a sinusoidal density wave with wavelength $2\pi/q$. This result is consistent with the de Gennes theory.

We should make four remarks about this free energy. First, $\hat{\mathbf{n}}$ only enters through the second-rank tensor $n_i n_j$, which corresponds to Q_{ij} in Refs. [6–8]. Hence, the free energy depends only on $n_i n_j$ and $\delta\rho$, which are both physical, single-valued functions, with no need for branch cuts. Second, the free energy includes a third-order term of $\delta\rho^3$. This term is allowed because there is no symmetry between high density ($\delta\rho > 0$) and low density ($\delta\rho < 0$). Third, it could include other terms permitted by symmetry, such as $|\nabla\delta\rho|^2$ and $(\hat{\mathbf{n}}\cdot\nabla\delta\rho)^2$. These terms shift the nematic-SmA transition and the wavelength of the smectic density modulation, but do not change the general physics discussed here, so we will not consider them further. Fourth, it includes the nematic free energy density f_N. We use the simplest approximation $f_N = \frac{1}{2}K(\partial_i n_j)^2$ with a single Frank elastic constant, although it could be generalized to different Frank constants.

In the rest of this paper, we use the free energy (3) to calculate the director orientation and layer configuration in two-dimensional SmA liquid crystals. We consider a SmA phase confined inside a small domain with boundary conditions requiring defects, and determine the lowest-energy structure. These calculations demonstrate the feasibility of our density-functional theory, and may be useful for designing devices with smectic liquid crystals under nanoscale confinement [17].

To calculate the ground state, we numerically minimize the free energy using Monte Carlo simulated annealing. The system is discretized using a quasi-regular uniform Delaunay triangulation. Its state is described by the director orientation and density at each vertex. The total free energy is calculated as a sum of free energies of all Delaunay cells. The free energy of each cell depends on first partial derivatives of the director and second partial derivatives of density with respect to position. The required derivatives are approximated by linear combinations of the variables at neighboring vertices.

To calculate the director and its first derivatives in each cell, we linearly interpolate each director component between the three vertices. The director at the cell's center is determined by interpolation and then normalized to unit length. To calculate the density and its second derivatives in each cell, we assume the density depends quadratically on the coordinates. Interpolation of the quadratic function between the closest six vertices gives the required derivatives and the density at the center.

In the Monte Carlo simulated annealing, trial director and density changes at any vertex change the free energy in all neighboring Delaunay cells, and in cells that use the vertex for calculating density derivatives. Thus, for each change of director or density at a vertex, the free energy is recalculated for several neighboring cells.

To analyze the numerical results, we want to describe the degree of smectic order as a function of position. For this purpose, we need the magnitude of density modulation at the wavelength corresponding to smectic layers. The simplest representation for this order parameter is a local Fourier transform of the density near any point, at the wave vector q along the local director,

$$S_A(\mathbf{r}) = \frac{q}{2\pi}\left|\int_{-\pi/q}^{\pi/q} e^{-iql}\rho(\mathbf{r}+\mathbf{n}l)dl\right|. \qquad (4)$$

This quantity is calculated by numerical integration and presented as the smectic order parameter in the figures below.

For an initial simulation to illustrate the difference between working with $\delta\rho(\mathbf{r})$ and working with $\psi(\mathbf{r})$, we consider a geometry with two half-charged disclinations. In this initial simulation, we assume the director field is held fixed and calculate the resulting smectic layer configuration. When we do this calculation using the free energy (3), expressed in terms of $\delta\rho(\mathbf{r})$, we obtain the structure shown in Fig. 2b. This structure is consistent with all the symmetries of the SmA phase. The layers are equally spaced and normal to the director everywhere. The region between the disclinations is a well-ordered smectic phase with no line defect.

By comparison, to illustrate the potential problems with using $\psi(\mathbf{r})$ and $Q_{ij}(\mathbf{r})$, we perform analogous simulations using the free energy density from Ref. [6], similar

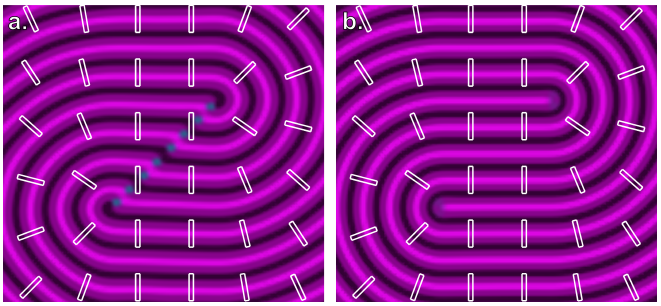

FIG. 2. Simulation of smectic layers using a fixed director field (shown by short lines) with two half-charged disclinations. (a) Results using the free energy (5), expressed in terms of $\psi(\mathbf{r})$, with parameters $\alpha = -1$, $\beta = 100$, $b_1 = -3$, $b_2 = 5$, $e_1 = -b_1 - 8b_2(\pi/10)^2$. (b) Results using the free energy (3), expressed in terms of $\delta\rho(\mathbf{r})$, with parameters $a = -0.1$, $b = 0$, $c = 10$, $q = 2\pi/10$, $B = 0.1/q^4$.

to Ref. [11],

$$f = \frac{1}{2}\alpha|\psi|^2 + \frac{1}{4}\beta|\psi|^4 + \frac{2b_1 - e_1}{4}|\nabla_i\psi|^2 + \frac{1}{2}b_2|\Delta\psi|^2 + \frac{3}{4}e_1 n_i n_j \nabla_i\psi\nabla_j\psi^* + \frac{1}{2}K(\partial_i n_j)(\partial_i n_j). \qquad (5)$$

As a simplification, we assume here that the magnitude of nematic order is constant, so that $Q_{ij} = \frac{3}{2}n_i n_j - \frac{1}{2}\delta_{ij}$, and use the single elastic constant approximation. We perform these simulations on a square lattice with derivatives approximated by standard finite differences. The results are shown in Fig. 2a. Here, the color indicates $|\psi|$ (with purple and blue representing higher and lower order, respectively), while the brightness indicates $Re(\psi)$ (giving the local density). Note that this simulation shows a line defect connecting the two disclinations. This line defect is a specific example of the branch cut discussed earlier: a boundary where $\nabla\psi \to \nabla\psi^*$. As an artifact of the model, this boundary has a free energy penalty, which is linearly proportional to the distance between disclinations and hence binds the disclinations together. To minimize the free energy, the algorithm shifts some of the penalty from $Im(\psi)$ to $Re(\psi)$, and hence it appears as a line defect in the density wave. That line defect is unphysical, because there is no need for any line defect there; the density wave can have a smooth curvature as calculated through density functional theory.

For a second example, we perform simulations where the director field and layer configuration can both relax. We consider the circular geometry shown in Fig. 3, with boundary conditions on the director requiring a single half-charged disclination. Subject to that constraint, the director and layers relax together inside the domain.

When we do the calculation with the free energy (3), using $\delta\rho(\mathbf{r})$, we obtain the structure shown in Fig. 3b, which has a single half-charged disclination at the center. The smectic layers form a relaxed configuration about the disclination. There is a point defect in the layers at

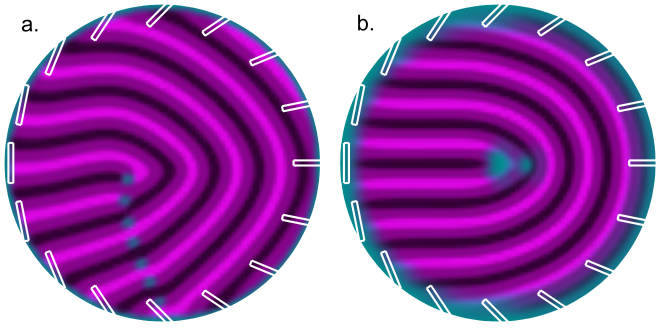

FIG. 3. Simulations of a circular domain with boundary conditions requiring a single half-charged disclination. (a) Results using the free energy (5), with parameters $\alpha = -1$, $\beta = 100$, $b_1 = -3$, $b_2 = 5$, $e_1 = -b_1 - 8b_2(\pi/10)^2$, $K = 0.0025$. (b) Results using the free energy (3), with parameters $a = -0.1$, $b = 0$, $c = 10$, $q = 2\pi/10$, $B = 0.1/q^4$, $K = 0.008$.

the disclination core, where we can see a reduction in the smectic order parameter defined by the local Fourier transform. Everywhere else, the layers are well-ordered and equally spaced.

By comparison, when we do the calculation with the free energy (5), using $\psi(\mathbf{r})$, we obtain the structure shown in Fig. 3a. Once again, we see a line defect in the layers coming out of the disclination. Because there is no other disclination where the line defect can terminate, it runs all the way to the boundary. This line defect is not required by the symmetry of the smectic phase; it is just an artifact of the complex order parameter formalism.

For further examples of the density functional theory, we perform simulations of the circular domains shown in Fig. 4. Here, the director field has tangential boundary conditions (parts a and b) or radial boundary conditions (c and d). In either case, it must have total topological charge of +1. The density modulation has free boundary conditions. We use two values of the Frank elastic constant K compared to the nematic-smectic coupling B, and hence two values of the length scale $\lambda = (K/B)^{1/2}$. This characteristic smectic length scale is large in a and c, and smaller in b and d. In all cases, free energy minimization gives a configuration with two disclinations of topological charge +1/2 each, *not* a single disclination of +1. In the two cases with high λ, the director has a smooth variation between the disclinations, and the layers adapt to the director, with small variations in the layer spacing. In the two cases with smaller λ, the layers are equally spaced over most of the domain, and the director adapts to the layers, with director variation concentrated in small regions near the boundary. These results are physically reasonable, and correspond to what might be observed for smectic liquid crystals under nanoscale confinement [17].

As a final point, we note that the complex order parameter formalism has a second problem, albeit less severe

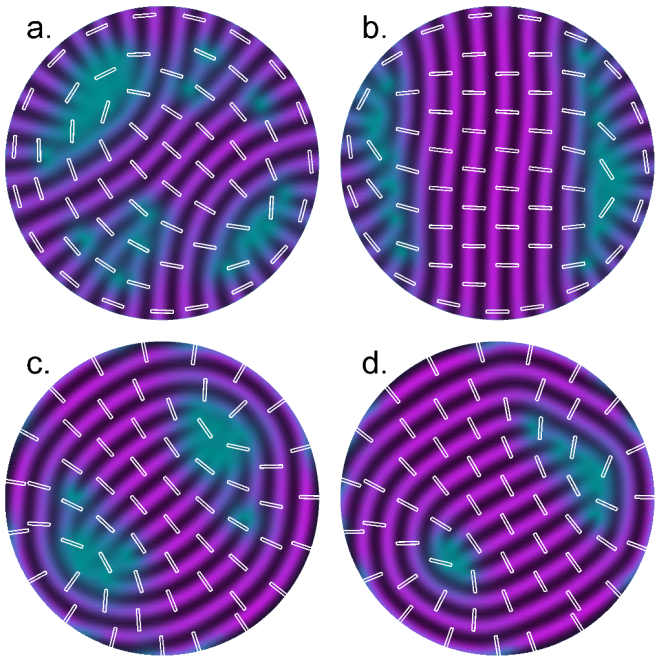

FIG. 4. Simulations of a circular domain with boundary conditions requiring tangential alignment (parts a and b) or radial alignment (c and d) of the director. The density functional free energy (3) is used. In a and c, parameters are $a = -5$, $b = 0$, $c = 5$, $B = 10^{-5}$, $q = 40$, $K = 0.3$. In b and d, the Frank constant is reduced to $K = 0.05$.

than the line defects discussed above. In this formalism all positions are equivalent, with the same free energy density, regardless of whether they are density maxima, minima, or anywhere in between. For that reason, a dislocation in the smectic layers is equally likely to occur anywhere within the layer structure. As a result, there is no Peierls-Nabarro energy barrier for dislocation glide from layer to layer, the process illustrated in Fig. 9.17 of Ref. [22]. Indeed, if we multiply $\psi(\mathbf{r})$ by a *uniform* phase factor $e^{i\phi}$, we explicitly shift the layers with respect to the defect position, and obtain dislocation glide at zero energy cost. This symmetry is unphysical: in the real system, the density maxima and minima are special positions, and there must be some free energy difference between defects at those positions and defects at other positions. The density formalism shows these special positions explicitly, and hence predicts a nonzero Peierls-Nabarro barrier for dislocation glide [23].

In conclusion, we have identified a problem with the complex order parameter formalism for modeling smectic liquid crystals, which affects calculations that should be able to produce half-charged disclinations. We have discussed three ways to solve this problem: canceling the branch cut in the smectic order parameter with another branch cut in the nematic director, defining a new type of mathematical object for the smectic order parameter, or working with the physical density variation $\delta\rho$. All three

of these approaches should be possible, but the third approach seems to us the simplest and most physical, and it has the further advantage of a nonzero Peierls-Nabarro barrier. We have demonstrated that it works for sample geometries, and it has potential for future design of nanoscale smectic devices.

For helpful discussions we thank M. Linehan, who reached related conclusions by a different route, and B. R. Ratna, who provided experimental motivation for this study. Some of this work was carried out at the Isaac Newton Institute for Mathematical Sciences, Cambridge, UK, which we thank for its hospitality. This work was supported by NSF Grants DMR-0605889 and 1106014.

* jselinge@kent.edu
† T.J.Sluckin@soton.ac.uk

[1] P.-G. de Gennes, Solid State Comm. **10**, 753 (1972).
[2] P.-G. de Gennes, *The Physics of Liquid Crystals* (Clarendon Press, Oxford, 1974).
[3] B. I. Halperin and T. C. Lubensky, Solid State Comm. **14**, 997 (1974).
[4] B. I. Halperin, T. C. Lubensky, and S.-K. Ma, Phys. Rev. Lett. **32**, 292 (1974).
[5] J.-H. Chen, T. C. Lubensky, and D. R. Nelson, Phys. Rev. B **17**, 4274 (1978).
[6] P. Mukherjee, H. Pleiner, and H. Brand, Eur. Phys. J. E **4**, 293 (2001).
[7] P. Mukherjee and F. Giesselmann, J. Chem. Phys. **121**, 12038 (2004).
[8] P. Biscari, M. C. Calderer, and E. M. Terentjev, Phys. Rev. E **75**, 051707 (2007).
[9] S. R. Renn and T. C. Lubensky, Phys. Rev. A **38**, 2132 (1988).
[10] N. M. Abukhdeir and A. D. Rey, Solid State Phenomena **139**, 135 (2008).
[11] N. M. Abukhdeir and A. D. Rey, New J. Phys. **10**, 063025 (2008).
[12] N. M. Abukhdeir and A. D. Rey, Macromolecules **42**, 3841 (2009).
[13] N. M. Abukhdeir and A. D. Rey, Langmuir **25**, 11923 (2009).
[14] N. M. Abukhdeir and A. D. Rey, Liquid Crystals **36**, 1125 (2009).
[15] E. R. Soule, N. M. Abukhdeir, and A. D. Rey, Macromolecules **42**, 9486 (2009).
[16] N. M. Abukhdeir and A. D. Rey, Soft Matter **6**, 1117 (2010).
[17] C. M. Spillmann, J. Naciri, K. J. Wahl, Y. H. Garner, M.-S. Chen, and B. R. Ratna, Langmuir **25**, 2419 (2009).
[18] G. P. Alexander, B. G.-g. Chen, E. A. Matsumoto, and R. D. Kamien, Phys. Rev. Lett. **104**, 257802 (2010).
[19] G. P. Alexander, R. D. Kamien, and C. D. Santangelo, Phys. Rev. Lett. **108**, 047802 (2012).
[20] A. Poniewierski and T. J. Sluckin, Phys. Rev. A **43**, 6837 (1991).
[21] A. Linhananta and D. E. Sullivan, Phys. Rev. A **44**, 8189 (1991).
[22] M. Kleman and O. D. Lavrentovich, *Soft Matter Physics: An Introduction* (Springer-Verlag, New York, 2003).
[23] See the Supplemental Material for explicit numerical calculations of the energy of an edge dislocation, as a function of its position with respect to the layer structure, using the complex order parameter formalism and the real density formalism.

SUPPLEMENTAL MATERIAL

This note presents explicit numerical calculations of the energy of an edge dislocation in the 2D SmA phase, using the two theoretical approaches discussed in the Letter. In the complex order parameter formalism, the dislocation energy is independent of position with respect to the layer structure, and hence there is no Peierls-Nabarro energy barrier for dislocation glide. By contrast, in the real density formalism, the dislocation energy depends on position and the Peierls-Nabarro barrier is nonzero, as is physically realistic.

In the 2D (x, y) plane, the local density is given by $\rho(x, y) = \rho_0 + \delta\rho(x, y)$, which is related to the complex order parameter by $\delta\rho(x, y) = Re[\psi(x, y)]$. To describe a single edge dislocation, we choose the complex order parameter $\psi(x, y) = e^{i(qy+\Phi(x,y)+\Delta\Phi)}$, where $\Phi(x, y) = \arg(x + iy)$ is the phase variation and $\Delta\Phi$ is a constant phase offset. The director $\hat{\mathbf{n}}(x, y)$ is chosen as a unit vector along the gradient of $\psi(x, y)$.

Figure 1 shows a visualization of $\Phi(x, y)$; the branch cut starts at $(x = 0, y = 0)$ and goes in positive x direction. The first column of pictures in Fig. 2 shows corresponding visualizations of the density variation around the dislocation. Note that the constant phase offset $\Delta\Phi$ defines the position of the dislocation with respect to the layer structure. When $\Delta\Phi = 0$ the dislocation occurs at a density minimum (shown in blue); when $\Delta\Phi = \pi$ it occurs at a density maximum (shown in red). For intermediate $\Delta\Phi$ it occurs at a lower-symmetry point between those extremes.

In the complex order parameter formalism, the free energy density is given by

$$f(\psi) = r|\psi|^2 + \frac{u}{2}|\psi|^4 + C|(\nabla - iq\hat{\mathbf{n}})\psi|^2. \qquad (1)$$

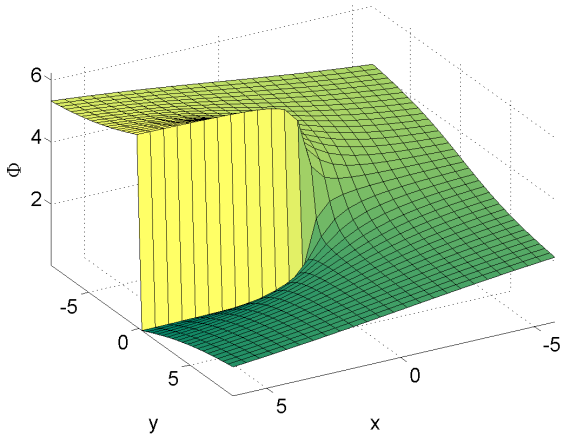

FIG. 1. Visualization of the phase variation $\Phi(x, y)$ around a single edge dislocation.

As a specific example, the second column of pictures in Fig. 2 shows the free energy density for the parameters $r = -5$, $u = 5$, $q = 1$, and $C = 1/q^2$. From these pictures, we can see that the free energy density is sharply peaked at the dislocation, and decays rapidly away from the dislocation. The free energy density of Eq. (1) is clearly independent of the constant phase offset $\Delta\Phi$, and indeed all the pictures in this column are identical. As a result, the integrated free energy is also independent of $\Delta\Phi$. This result implies that the dislocation can move with respect to the layer structure, from row to row in the table, with no energy cost. In the terminology of dislocation theory, we would say that the Peierls-Nabarro energy barrier for dislocation glide is zero. This result is physically unrealistic, and shows that the model has more symmetry than the actual SmA phase.

By comparison, in the real density formalism, the free energy density is given by

$$f(\delta\rho) = \frac{a}{2}\delta\rho^2 + \frac{b}{3}\delta\rho^3 + \frac{c}{4}\delta\rho^4 + B\left[(\partial_i\partial_j + q^2 n_i n_j)\delta\rho\right]^2. \qquad (2)$$

For specific examples, the third and fourth columns of pictures in Fig. 2 show the free energy density calculated for the parameters $a = -10$, $c = 10$, $q = 1$, $B = 0.1/q^4$, and $b = 0$ (in the third column) and $b = 1$ (in the fourth column). The b term is important because it is the only term considered here that is odd in $\delta\rho$, and hence the only term that distinguishes between density minima and maxima. From these images, we can make several observations. First, the free energy density is not uniform but periodic in the smectic layer structure. If $b = 0$, there are equal free energy valleys at the density minima and maxima. If $b > 0$, the symmetry between minima and maxima is broken (as is physically realistic), and the deepest free energy valleys are at the density minima. Furthermore, there is additional free energy associated with the dislocation itself. Most importantly, the free energy plots change as the constant phase offset $\Delta\Phi$ is varied, i. e. as the dislocation moves with respect to the layer structure. Hence, this model does not have the unphysical symmetry found in the complex order parameter formalism.

To calculate the barrier for dislocation motion, we must integrate the free energy density to find the total free energy as a function of $\Delta\Phi$. In this calculation, it is important to integrate over an integer number of layers, so that the result is not influenced by the number of fractional layers within the integration region. Hence, we define the integration region by $|qx| < 10\pi$ and $|qy + \Phi(x, y)| < 8\pi$, as shown in Fig. 3.

Figure 4 presents graphs of the total free energy as a function of $\Delta\Phi$. We can see that it has a periodic series of peaks and valleys as the dislocation moves with respect to the layer structure. If $b = 0$, the valleys occur whenever

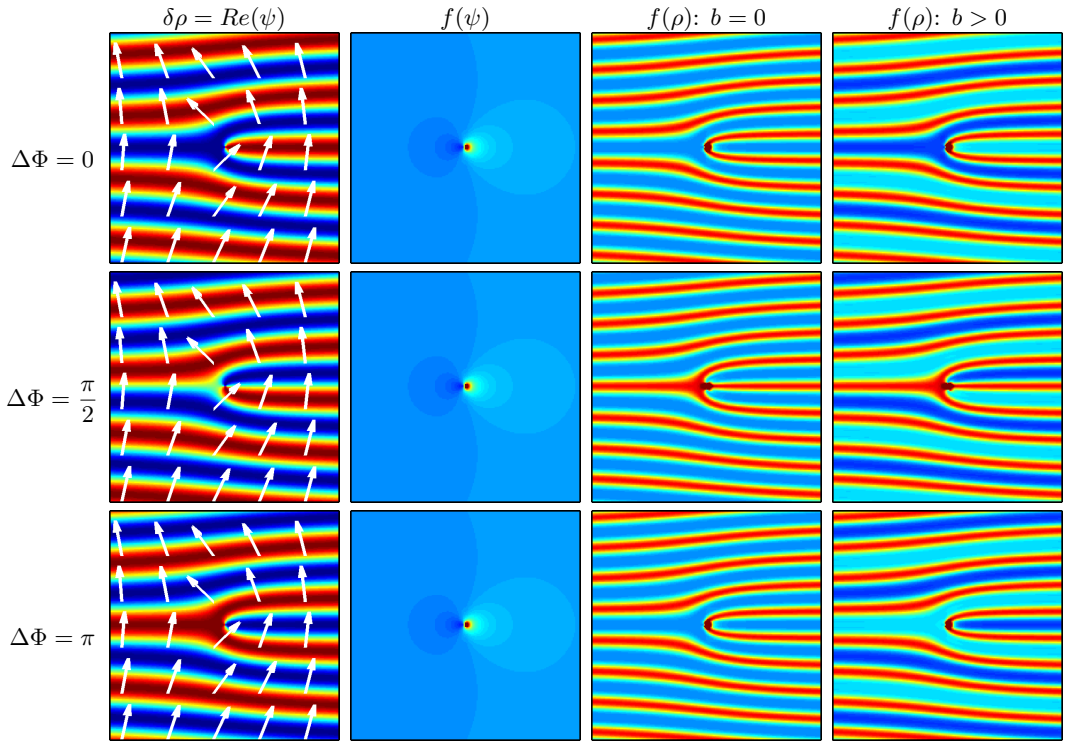

FIG. 2. Behavior as the dislocation is displaced with respect to the layer structure. Plots show the smectic density variation, the free energy density for the complex order parameter formalism, and the free energy density for the real density formalism (calculated for the cubic parameter $b = 0$ and $b \neq 0$). Red represents highest values of density or free energy; blue represents lowest values.

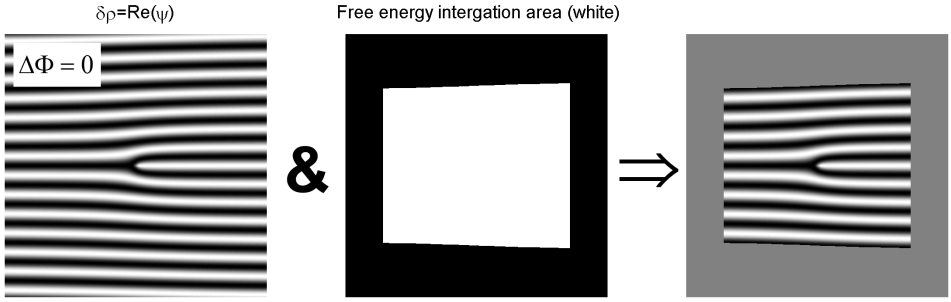

FIG. 3. Integration of the free energy density over a region containing an integer number of smectic layers.

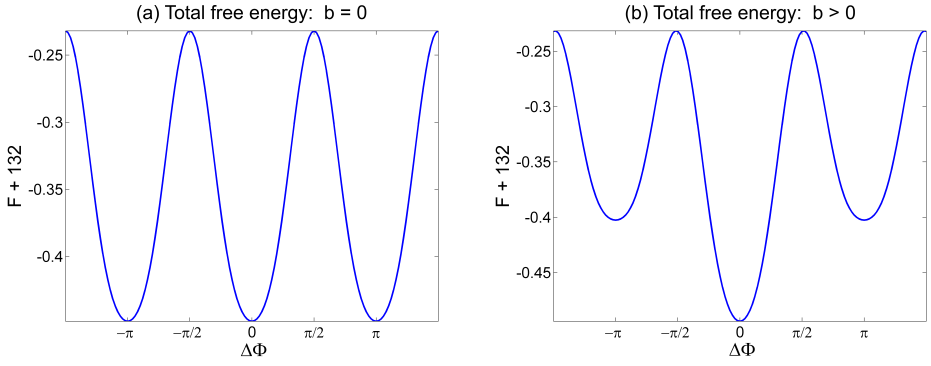

FIG. 4. Integrated free energy in the real density formalism as the dislocation is displaced with respect to the layer structure, as given by the parameter $\Delta\Phi$. (a) Parameters $a = -10$, $c = 10$, $q = 1$, $B = 0.1/q^4$, and $b = 0$, so that there is a symmetry between density minima and maxima. (b) Parameter $b = 1$, breaking the symmetry between density minima and maxima.

$\Delta\Phi$ is a multiple of π, i. e. whenever the dislocation is at either a density minimum or maximum. If $b > 0$, the deepest valleys occur when $\Delta\Phi$ is a multiple of 2π, i. e. when the dislocation is at a density minimum; the valleys at density maxima are less deep. The Peierls-Nabarro energy barrier for dislocation glide is then the difference in free energy between the deepest valleys and highest peaks in this plot.